

## Technical Information

# Estimating Mass Concentration Using a Low-cost Portable Particle Counter Based on Full-year Observations: Issues to Obtain Reliable Atmospheric PM<sub>2.5</sub> Data

Sayako Ueda<sup>1),2),\*</sup>, Kazuo Osada<sup>1)</sup>, Makiko Yamagami<sup>3)</sup>, Fumikazu Ikemori<sup>3)</sup>, Kunihiro Hisatsune<sup>3)</sup>

<sup>1)</sup>Graduate School of Environmental Studies, Nagoya University, Furo-cho, Chikusa-ku, Nagoya, Aichi 464-8601, Japan

<sup>2)</sup>Japan Society for the Promotion of Science, Kojimachi, Chiyoda-ku, Tokyo 102-0083, Japan

<sup>3)</sup>Nagoya City Institute for Environmental Sciences, 5-16-8 Toyoda, Minami-ku, Nagoya, Aichi 457-0841, Japan

**\*Corresponding author.**

Tel: +81-52-789-4306

E-mail: [ueda.sayako@d.mbox.nagoya-u.ac.jp](mailto:ueda.sayako@d.mbox.nagoya-u.ac.jp)

Received: 25 September 2019

Revised: 30 January 2020

Accepted: 7 April 2020

**ABSTRACT** Expanding the use of a recently introduced low-cost particle monitor (DC1700 Dylos Air Quality Monitor) for sensing atmospheric PM<sub>2.5</sub> requires comparison with data obtained using a certified method for PM<sub>2.5</sub> based on appropriate atmospheric observations. Full-year measurements of atmospheric aerosols were taken in Nagoya, Japan during March 2017–March 2018 using the DC1700 to measure the particle number concentrations of >0.5 and >2.5 μm diameter particles and to measure the PM<sub>2.5</sub> mass concentration ( $M_{\text{dry, PM}_{2.5}}$ ) using an automated β attenuation mass monitor (PM712). The number-size distribution was measured using an optical particle counter (KC01D). The dried mass concentration of 0.5–2.5 μm particles ( $M_{\text{dry, 0.5-2.5}}$ ) was estimated from the ambient relative humidity and the DC1700 number concentration. The values of  $M_{\text{dry, 0.5-2.5}}$  were invariably less than those of  $M_{\text{dry, PM}_{2.5}}$ . The coefficient of determination and slope of  $M_{\text{dry, 0.5-2.5}}$  to  $M_{\text{dry, PM}_{2.5}}$  for the year were, respectively, 0.68 and 0.40. Slope values changed seasonally from 0.24 in July and August 2017 to 0.55 in May and April 2017. Light absorbing particles, smaller-fine particles, and the estimation method of  $M_{\text{dry, 0.5-2.5}}$  were inferred as causes of the difference between  $M_{\text{dry, 0.5-2.5}}$  and  $M_{\text{dry, PM}_{2.5}}$ . Especially, we estimated a large contribution (ca. 54% underestimation of  $M_{\text{dry, 0.5-2.5}}$  into  $M_{\text{dry, PM}_{2.5}}$ ) of particles smaller than the minimum detection diameter of DC1700. The seasonal variation of  $M_{\text{dry, 0.5-2.5}}/M_{\text{dry, PM}_{2.5}}$  was related to the volume fraction of particles smaller than 0.5 μm. Good correlation of  $M_{\text{dry, 0.5-2.5}}$  to  $M_{\text{dry, PM}_{2.5}}$  suggests that data obtained using DC1700 with a correction factor are useful as a rough proxy of atmospheric PM<sub>2.5</sub> within a season. However, precise estimation of PM<sub>2.5</sub> from the DC1700 number concentrations should include appropriate corrections of the size distribution, not only hygroscopicity.

**KEY WORDS** Atmospheric aerosols, Dylos, Low-cost monitor, Optical sensor, PM<sub>2.5</sub>

## 1. INTRODUCTION

Atmospheric aerosol particles have been studied extensively because of their important role in assessing air quality and Earth climate. Fine particulate matter has been recognized as adversely affecting human health, leading to premature mortality in many people (Zhang *et al.*, 2017; Lelieveld *et al.*, 2015). Among fine particles, those with aerodynamic diameter less than 2.5 μm are defined as PM<sub>2.5</sub>.

Actually, PM<sub>2.5</sub> mass concentrations have been monitored widely using various instruments based on tapered-element oscillating microbalances, beta attenuation, and a hybrid of beta attenuation and light scattering, in conjunction with an impactor or a cyclone at the inlet (EPA, 2013; Kulkarni *et al.*, 2011).

Recently, low-cost monitors of PM<sub>2.5</sub> have received increasing attention for measuring temporal and spatial concentration variations in indoor and outdoor environments (Rai *et al.*, 2017; Jovašević-Stojanović *et al.*, 2015; Kumar *et al.*, 2015). Particularly developed have been instruments with optical sensors that detect light scattered from particles. Their use has expanded rapidly because of their low cost, compact size, and high time resolution (Liu *et al.*, 2017; Nakayama *et al.*, 2017; Zikova *et al.*, 2017; Jiao *et al.*, 2016; Austin *et al.*, 2015). Although some points of caution have been indicated, such as the need for correction under high humidity conditions (Jayaratne *et al.*, 2018; Zheng *et al.*, 2018; Han *et al.*, 2017), many reports have described good correlation between output values from these devices and PM<sub>2.5</sub> mass concentrations measured using conventional methods (Johnson *et al.*, 2018; Kelly *et al.*, 2017; Nakayama *et al.*, 2017; Rai *et al.*, 2017; Zikova *et al.*, 2017). Such low-cost monitors, because of their beneficial characteristics of mobility and time-resolution, offer great potential for use in many situations such as investigation of streets and building environments.

Results obtained using the two-channel (>0.5 μm and >2.5 μm) optical particle counters (DC1100 and DC1700; Dylos Corp.) adopted for this study have been compared widely with PM<sub>2.5</sub> mass concentrations measured in atmospheric, laboratory, and closed environments (Rai *et al.*, 2017; Jones *et al.*, 2016; Manikonda *et al.*, 2016; Sousan *et al.*, 2016; Dacunto *et al.*, 2015; Semple *et al.*, 2013). Earlier reports have described good correlation between PM<sub>2.5</sub> mass concentration and outputs from DC series. The device is sold at a reasonable price. Therefore, we expect that the device can be used easily for measuring PM<sub>2.5</sub> at various sites to provide multi-point and high-time-resolution data. Nevertheless, the light scattering intensity differs depending on the optical properties of aerosol species such as dust, sea salt, and diesel fumes (Sousan *et al.*, 2016). Atmospheric aerosols have various size distributions and compositions, which differ by time and location. Such aerosol physicochemical properties can affect their optical properties. Therefore, detection sensitivities of optical sensors vary accor-

ding to time and location. Using data from a particle counter as a proxy of atmospheric PM<sub>2.5</sub> therefore requires knowledge of the reliability and limitations of measurements. Although one report has described comparison with PM<sub>2.5</sub> mass concentration (Han *et al.*, 2017), the observation periods used for that study were less than 1 month. Moreover, they covered few seasons. A shorter observation duration makes it difficult to detect variation according to various parameters. Therefore, realistic evaluation of optical responses is difficult. For another low-cost sensor PMS, Sayahi *et al.* (2019) and Zheng *et al.* (2018) evaluated the performance for measuring PM<sub>2.5</sub> mass concentrations based on long-term observations. They reported seasonal differences in sensor performance. Zheng *et al.* (2018) compared the sensor performance to meteorological parameters, especially relative humidity. However, the relation of the performance with seasonal/event changes of atmospheric aerosol properties such as light absorbing aerosols and size distribution was not explained. For these reasons, data obtained using a low-cost monitor should be compared for at least one year to those obtained from a certified PM<sub>2.5</sub> monitor with aerosol properties.

For this study, simultaneous measurements obtained using one optical particle counter (DC1700; Dylos Corp.) were used to compile particle number concentrations of >0.5 and >2.5 μm diameter particles for comparison with PM<sub>2.5</sub> data obtained based on β attenuation method during one year in Nagoya, Japan. Most earlier studies using data obtained using a DC1700 had evaluated the correlation coefficient and regression formula for PM<sub>2.5</sub> mass concentrations directly from the number concentration (Rai *et al.*, 2017; Manikonda *et al.*, 2016; Sousan *et al.*, 2016; Dacunto *et al.*, 2015; Semple *et al.*, 2013). However, the degree of undercounting or overcounting by DC1700 was less apparent when using the earlier method. In the present study, to evaluate underestimation and overestimation of PM<sub>2.5</sub> and temporal variation more quantitatively, the mass concentration of particles counted by the DC1700 was estimated and compared to the PM<sub>2.5</sub> mass concentration. Several studies have demonstrated the necessity of considering aerosol hygroscopicity. Therefore, we clarified the long-term difference originated in other factors by estimation of the mass concentration after humidity correction. Special attention is devoted to factors affecting uncertainty derived from temporal changes in the number-size distribution.

## 2. MEASUREMENTS AND DATA TREATMENTS

### 2.1 Observation Sites and Instruments

Table 1 presents locations and instrumentation used for this study. Simultaneous observations were made using the DC1700 device and standard monitor of PM<sub>2.5</sub> at the Nagoya City Institute for Environmental Sciences (NCIES) located in Nagoya city, central Japan, during March 2017–March 2018. Fig. 1 portrays a location map of the observation sites in Nagoya, a major city with about 2.3 million residents. Yamagami *et al.* (2019) reported details of NCIES and PM<sub>2.5</sub> measurements at the site. The air mass at the site is often affected by long-range transport from continental eastern Asia in addition to domestic emissions. Particle diameters detected using the DC1700 show separation at  $> 0.5 \mu\text{m}$  and  $> 2.5 \mu\text{m}$ . The DC1700 was put in a weather shield box fitted with air ducts passing outside air easily. The weather shield box was installed outdoors under eaves to prevent sunlight and rain exposure. Hourly PM<sub>2.5</sub> mass concentrations were monitored using a  $\beta$  attenuation mass monitor (PM712; Kimoto Electric Co. Ltd.) installed in an outdoor case on the flat roof of the NCIES building. The PM712 is a PM<sub>2.5</sub> automatic measuring instrument that uses the standard method accepted in Japan. The temperature and relative humidity of the sample air and ambient air were measured respectively downstream of a

PTFE tape filter and outside of the outdoor case. The PM712 also measured the mass concentration of optical black carbon (OBC,  $M_{\text{OBC}}$ ) based on attenuation of near-IR scattering on a sampling spot of PM<sub>2.5</sub>. Daily samples of PM<sub>2.5</sub> were collected using a pair of FRM-2000 samplers (Rupprecht and Patashnick Co. Inc., Albany, NY, USA) with PTFE filters (TK15-G3M; Pall Corp., Port Washington, NY, USA) for ion components and quartz fiber filters (2500QATUP; Pall Corp.) for carbon at NCIES. These samples were collected from 10:00 a.m. through 9:30 a.m. the next day. Details of FRM samplers at NCIES were reported by Ueda *et al.* (2016) and by Yamagami *et al.* (2019). Although original data obtained using the DC1700 were recorded every minute, their hourly averages were used for comparison with PM<sub>2.5</sub> mass concentrations.

The number-size distribution of aerosol particles, which was measured continually at Nagoya University (NU), was also used to evaluate data at NCIES. The distance between NCIES and NU is about 8 km (Fig. 1). The number-size distributions were measured using an optical particle counter (KC01D; Rion Co. Ltd.) with a laser diode. The KC01D measured the number concentrations for particles larger than 0.3, 0.5, 1.0, 2.0, and 5.0  $\mu\text{m}$  diameter. The irradiated volume  $v$  of the laser was  $5.0 \times 10^{-4} \text{cm}^3$ . Sample air was introduced into the KC01D located in the observation room of the seventh floor after drying in a diffusion dryer to less than

**Table 1.** Locations and instruments discussed.

Station	Nagoya City Institute for Environmental Sciences (NCIES)	Nagoya University (NU)	National air monitoring station in Nagoya at Kanokoden (KNK)
Location	35.10°N, 136.92°E, 0 m a.s.l.	35.16°N, 136.97°E, 49 m a.s.l.	35.18°N, 136.98°E, 59 m a.s.l.
Direction and distance from NCIES	–	Northeast, about 8 km	Northeast, about 9 km
Instrument	DC1700 Number concentrations of > 0.5, > 2.5 $\mu\text{m}$	DC1700 Number concentrations of 0.5, > 2.5 $\mu\text{m}$	ACSA Mass concentration of PM <sub>2.5</sub>
	PM712 Mass concentration of PM <sub>2.5</sub> OBC mass concentration of PM <sub>2.5</sub> RH and Temp. of ambient and sample air	KC01D Number concentrations of > 0.3, > 0.5, > 1.0, > 2.0, > 5.0 $\mu\text{m}$	
	FRM-2000 Mass concentration of PM <sub>2.5</sub>		
Period	Mar. 2017–Mar. 2018	Mar. 2017–Mar. 2018	Apr. 2017–Mar. 2018

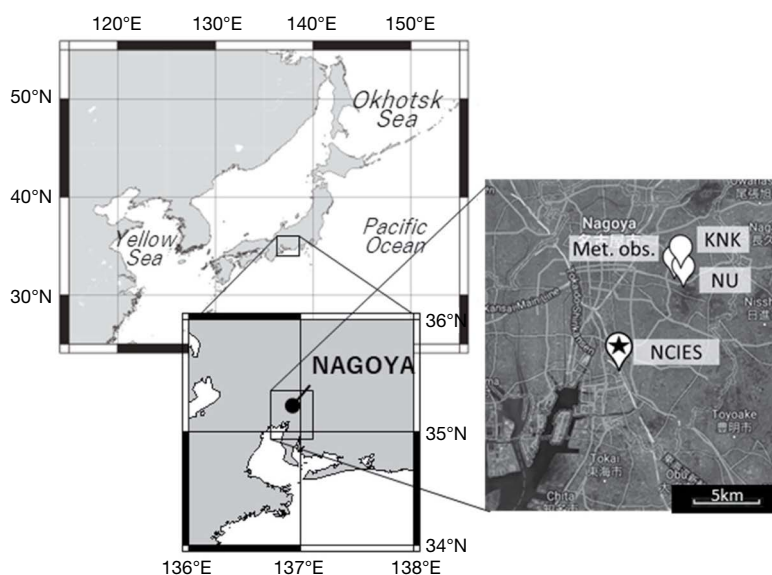


**Fig. 1.** Map showing locations of observation sites (Nagoya City Institute for Environmental Sciences (NCIES), Nagoya University (NU), National air monitoring station in Nagoya at Kanokoden (KNK), and the local meteorological observatory (Met. Obs.) in Nagoya, Japan.

20% relative humidity (RH). The length of tubing from the inlet to KC01D was about 3 m. The sample air flow rate was  $0.5 \text{ L min}^{-1}$ . A diffusion dryer used to keep the sample RH below 20% consisted of a 20-cm-long, 7-cm-diameter acrylic pipe and two desiccants mainly consisting of magnesium chloride (Nisso Dry-M; Nisso Fine Co., Ltd.). The KC01D was replaced by another instrument of the same type for maintenance during 12 May 2017 and 8 December 2017 because of air flow clogging. The use of KC01D data was limited to evaluation of the relative change of particle size distribution. Data of the optical particle counter needed to be corrected for the loss for coincidence counting error, depending on  $\nu$  and the particle number concentration. For comparison to data at the NCIES, measurements using the DC1700 in a weather shield box were also conducted at NU. In addition,  $\text{PM}_{2.5}$  mass concentrations were monitored at the national air monitoring station in Nagoya at Kanokoden (KNK), which is near NU (within 2 km). Those data were used to evaluate regional differences of  $\text{PM}_{2.5}$  mass concentrations. From March 2017, the  $\text{PM}_{2.5}$  mass concentrations were measured hourly (ACSA-14; Kimoto Electric Co. Ltd.) using the same method as that used for PM712.

Hourly precipitation and temperature data were obtained from a local meteorological observatory at Nagoya. The distance from NCIES to KNK and the meteorological observatory is about 9 km (Fig. 1). The meteorologi-

cal observatory is also within 2 km of NU.

## 2.2 $\text{PM}_{2.5}$ Mass Concentration by PM712 and FRM

Mass concentrations of  $\text{PM}_{2.5}$  used for routine air monitoring such as the Federal Reference Method (FRM), which is widely regarded as reliable, were measured under the condition of  $35 \pm 5\%$  RH around the sample. PM712 provides the mass concentration of  $\text{PM}_{2.5}$  equivalent to the value of FRM after correcting the water contents of ambient particles (Kimoto Electric Co. Ltd., 2007).

$$\frac{M_{\text{total, PM}_{2.5}}}{M_{\text{dry, PM}_{2.5}}} = \frac{M_{\text{dry, PM}_{2.5}} + M_{\text{w, PM}_{2.5}}}{M_{\text{dry, PM}_{2.5}}} = 1 + a \times \exp\left(\frac{\text{RH}_{\text{sample}}}{100} \times b\right) \quad (1)$$

Therein,  $M_{\text{total, PM}_{2.5}}$ ,  $M_{\text{dry, PM}_{2.5}}$ , and  $M_{\text{w, PM}_{2.5}}$  respectively represent the mass concentrations of  $\text{PM}_{2.5}$  at the relative humidity of the sample air ( $\text{RH}_{\text{sample}}$ ), the mass concentration of dried  $\text{PM}_{2.5}$ , and the mass concentration of water contained in  $\text{PM}_{2.5}$  at  $\text{RH}_{\text{sample}}$ . In addition,  $a$  and  $b$  (respectively 0.010 and 6.000) are coefficients ascertained from correlations of daily data between the FRM and the PM712 obtained in Japan. A correction curve based on equation (1) for  $\text{RH} < 90\%$  is similar to a theoretical equation, assuming hygroscopicity of ammonium sulfate and ammonium nitrate (Iwamoto *et al.*, 2018; Snider *et al.*, 2016).

For equivalence checking of PM<sub>2.5</sub> mass concentration in this study, the PM<sub>2.5</sub> mass concentration found using PM712 at NCIES was compared with that estimated from daily sample of PM<sub>2.5</sub> by FRM. Fig. 2 presents scatter plots of daily PM<sub>2.5</sub> mass concentrations obtained using FRM and PM712 during the observation period. Daily PM<sub>2.5</sub> mass concentrations of PM712 were averaged for 24 hr of data obtained during 10:00 a.m. to 10:00 a.m. of the next day, using hourly data after correction by equation (1). Although plots for PM<sub>2.5</sub> mass concentration before humidity correction ( $M_{\text{total, PM}_{2.5}}$ ) show dispersion, the relation between PM<sub>2.5</sub> mass concentration by FRM and  $M_{\text{dry, PM}_{2.5}}$  showed good correlation of  $R^2 = 0.95$  and slope = 1.01. The greatest outlier plot (arrowed plot in Fig. 2) was that of data from a Kosa (dust) event of 7 May 2017. However, such cases were rarely observed. Most of the PM712 data showed a nearly 1:1 relation with those of FRM, suggesting that the daily average of mass concentration of PM<sub>2.5</sub> by PM712 after humidity correction using equation (1) was usually reliable to that by FRM. For this study, the hourly PM<sub>2.5</sub> mass concentration by PM712 was referenced to compare data of DC1700. The manufacturer states that averaged and standard deviations of hourly blanks of PM712 are within  $\pm 3.5 \mu\text{g m}^{-3}$  for more than 15 data. A recent report has described that PM<sub>2.5</sub> mass concentration by some instruments using  $\beta$  attenuation can have different

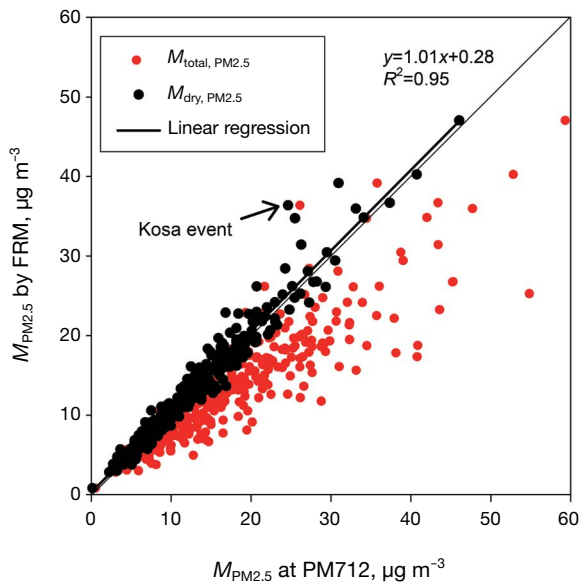


**Fig. 2.** Scatter plots of mass concentrations of PM<sub>2.5</sub> by PM712 and FRM at NCIES for the year of Mar. 2017 through Mar. 2018.

bias between night and daytime (Hasegawa *et al.*, 2018). However, their test for 12-hr samples using FRM showed good correspondence with the PM<sub>2.5</sub> mass concentration of PM712 in many cases, except at some times during daytime in winter.

### 2.3 Estimation of Mass Concentration from DC1700 Data

Based on the difference between particle number concentrations of  $> 0.5 \mu\text{m}$  and  $> 2.5 \mu\text{m}$  diameter obtained using DC1700, the number concentrations ( $N_{0.5-2.5}$ ) for  $0.5 \mu\text{m}$  to  $2.5 \mu\text{m}$  particles are calculable. The mass concentration ( $M_{0.5-2.5}$ ) for sizes of  $0.5 \mu\text{m}$  and  $2.5 \mu\text{m}$  was estimated from  $N_{0.5-2.5}$ , given as

$$M_{0.5-2.5} = \rho \frac{\pi}{6} D^3 N_{0.5-2.5} \quad (2)$$

where  $\rho$  and  $D$  respectively stand for the particle density and particle diameter. The  $D$  value was calculated as the geometric average between  $0.5 \mu\text{m}$  and  $2.5 \mu\text{m}$ . The  $\rho$  value was assumed for density ( $1.8 \text{ g/cm}^3$ ) of ammonium sulfate as the most abundant compound in PM<sub>2.5</sub> at Nagoya (Yamagami *et al.*, 2019; Ueda *et al.*, 2016; Ikemori *et al.*, 2015). According to their reports, sulfate, organic carbon, ammonium, elemental carbon, and nitrate were the major components, comprising more than 65% of the PM<sub>2.5</sub> mass concentration for all seasons. Chloride, sodium, potassium, magnesium, and calcium were less than 5% in PM<sub>2.5</sub>. Among the other densities of materials considered from major components, the respective densities of sulfuric acid and ammonium nitrate are 1.84 and  $1.73 \text{ g/cm}^3$ , which are similar values to those found for ammonium sulfate. The density of carbonaceous particles (approx.  $1.5 \text{ g/cm}^3$ ; Slowik *et al.*, 2004) is slightly lower than that of ammonium sulfate. Therefore, the value of  $M_{\text{dry, } 0.5-2.5}$  using the density of ammonium sulfate might be overestimated by as much as 17% under the condition that all particles are carbonaceous particles.

The value of  $M_{0.5-2.5}$  from DC1700 must be corrected for the hygroscopic increase of particle mass because measurements are conducted under ambient conditions without humidity control. For this study, the dried mass concentration ( $M_{\text{dry, } 0.5-2.5}$ ) obtained using the DC1700 was estimated, given as

$$M_{\text{dry, } 0.5-2.5} = M_{0.5-2.5} \left( 1 + a \times \exp \left( \frac{RH_{\text{ambient}}}{100} \times b \right) \right)^{-1} \quad (3)$$

where  $RH_{\text{ambient}}$  represents the relative humidity of ambient air. This correction uses the same method for PM712 as that shown in equation (1). Instead of  $RH_{\text{sample}}$  of equation (1),  $RH_{\text{ambient}}$  was applied to the correction for DC1700 because the length to the optical sensor in DC 1700 is short.

### 3. RESULTS AND DISCUSSION

#### 3.1 Temporal Variation of $M_{\text{dry}, 0.5-2.5}$ and $M_{\text{dry}, \text{PM}_{2.5}}$

Fig. 3 portrays temporal variations in March 2017 as an example of well-synchronized variation of  $M_{\text{dry}, \text{PM}_{2.5}}$  and  $M_{\text{dry}, 0.5-2.5}$ : (a) the number concentration of aerosol particles measured using DC1700 at NCIES and NU; (b)  $M_{\text{dry}, 0.5-2.5}$ ,  $M_{\text{dry}, \text{PM}_{2.5}}$ , and  $M_{\text{PM}_{2.5}}$  by FRM and  $M_{\text{dry}, 0.5-2.5}/M_{\text{dry}, \text{PM}_{2.5}}$  at NCIES; (c)  $M_{\text{OBC}}$  at NCIES; (d) the size-segregated volume concentration (0.3–5.0  $\mu\text{m}$ ) by KC01D at NU; (e) the relative humidity of ambient air measured at outside of PM712 ( $RH_{\text{ambient}}$ ) and downstream of the sample filter of PM712 ( $RH_{\text{sample}}$ ); and (f) the temperature and precipitation amounts recorded at the local meteorological observatory. The volume concentrations were calculated from the number concentrations for the respective size ranges of the KC01D, given as shown below.

$$V_{D_i-D_{i+1}} = \frac{\pi}{6} (D_i \cdot D_{i+1})^2 (N_i - N_{i+1}) \quad (4)$$

Therein,  $D_i$  and  $N_i$  respectively stand for the minimum particle diameter and number concentration of channel  $i$  counting for particles larger than  $D_i$  of KC01D.

As portrayed in Fig. 3a, the temporal variations of the number concentrations obtained using DC1700 at NU and NCIES were almost equal. Such synchronous variation was observed throughout the observation period. Fig. 4 presents a scatter plot of the number concentrations ( $>0.5 \mu\text{m}$  and  $>2.5 \mu\text{m}$ ) obtained by DC1700 at NCIES and NU and scatter plots of  $\text{PM}_{2.5}$  mass concentrations at NCIES and KNK for the observation periods. Their respective coefficients of determination ( $R^2$ ) and slope values of linear regression were 0.78–0.87 and 0.91–1.13. The good degree of correlation suggests that the air masses of these locations can be regarded as almost equivalent. As portrayed in Fig. 3b, the value of  $M_{\text{dry}, \text{PM}_{2.5}}$  was almost equal to that of  $M_{\text{PM}_{2.5}}$  by FRM. The temporal variation of  $M_{\text{dry}, 0.5-2.5}$  correlated well with that of  $M_{\text{dry}, \text{PM}_{2.5}}$  (Fig. 3b) and the volume concentration

(0.3–5.0  $\mu\text{m}$ ) obtained by KC01D (Fig. 3d). However, the values of  $M_{\text{dry}, 0.5-2.5}$  were always less than that of  $M_{\text{dry}, \text{PM}_{2.5}}$ : about 50% of  $M_{\text{dry}, \text{PM}_{2.5}}$  in March 2017. Also,  $RH_{\text{ambient}}$  was usually less than 80%, as depicted in Fig. 3e. The period of  $RH_{\text{ambient}}$  higher than 80% in the period was recorded during precipitation events (Fig. 3f). During such events,  $M_{\text{dry}, \text{PM}_{2.5}}$  tended to be lower. Higher  $M_{\text{dry}, \text{PM}_{2.5}}$  ( $>20 \mu\text{g m}^{-3}$ ) events were observed mostly under conditions of less than 70%  $RH_{\text{ambient}}$ . Although ambient and sample air humidity changed diurnally,  $M_{\text{dry}, 0.5-2.5}/M_{\text{dry}, \text{PM}_{2.5}}$  (Fig. 3b) is less dependent on humidity. The values of  $M_{\text{OBC}}$  (Fig. 3c) were usually less than 10% of  $M_{\text{dry}, \text{PM}_{2.5}}$ .

#### 3.2 Relation between $M_{\text{dry}, 0.5-2.5}$ and $M_{\text{dry}, \text{PM}_{2.5}}$

Scatter plots of  $M_{\text{dry}, \text{PM}_{2.5}}$  and  $M_{\text{dry}, 0.5-2.5}$  at NCIES for two months (a, March–April 2017; g, March 2018) and for all data in one plot (h) are presented in Fig. 5. The  $M_{\text{dry}, 0.5-2.5}$  values are shown below the 1 : 1 line to  $M_{\text{dry}, \text{PM}_{2.5}}$  values. The coefficient of determination ( $R^2$ ) and slope values of linear regression for all data in this study were, respectively, 0.68 and 0.40. Although the observation values for the whole period (Fig. 5h) showed large dispersion, the relations within two months (as shown in Figs. 5a, b, e and g) were found to have stronger correlation. For the scatter plot showing data of January and February (Fig. 5f), greater variation was apparent at higher concentrations during particular events in February (red dots in Figs. 5f and h), as discussed in section 3.4. The respective maximum and minimum values of  $R^2$  were 0.90 found for March–April 2017 (Fig. 5a) and 0.62 found for July–August (Fig. 5c) 2017. The respective maximum and minimum values of slopes were also 0.55 found for March–April 2017 and 0.24 found for July–August 2017. The slope values of linear regression differed by season. Fig. 6 portrays monthly box plots for ratios of  $M_{\text{dry}, 0.5-2.5}/M_{\text{dry}, \text{PM}_{2.5}}$  at NCIES. For March–April 2017 and December 2017–March 2018, the median values of  $M_{\text{dry}, 0.5-2.5}/M_{\text{dry}, \text{PM}_{2.5}}$  were 0.4–0.5. However, the median values were less than 0.4 for May–November 2017. They were especially low (approx. 0.25) in summer (July–August). The ratio of  $M_{\text{dry}, 0.5-2.5}/M_{\text{dry}, \text{PM}_{2.5}}$  decreased once in summer but recovered in winter and the following spring.

Han *et al.* (2017) also measured ambient aerosols using DC1700 in Houston, Texas. Correlation between the number concentration of 0.5–2.5  $\mu\text{m}$  and  $\text{PM}_{2.5}$  mass concentration found using standard instruments for 12

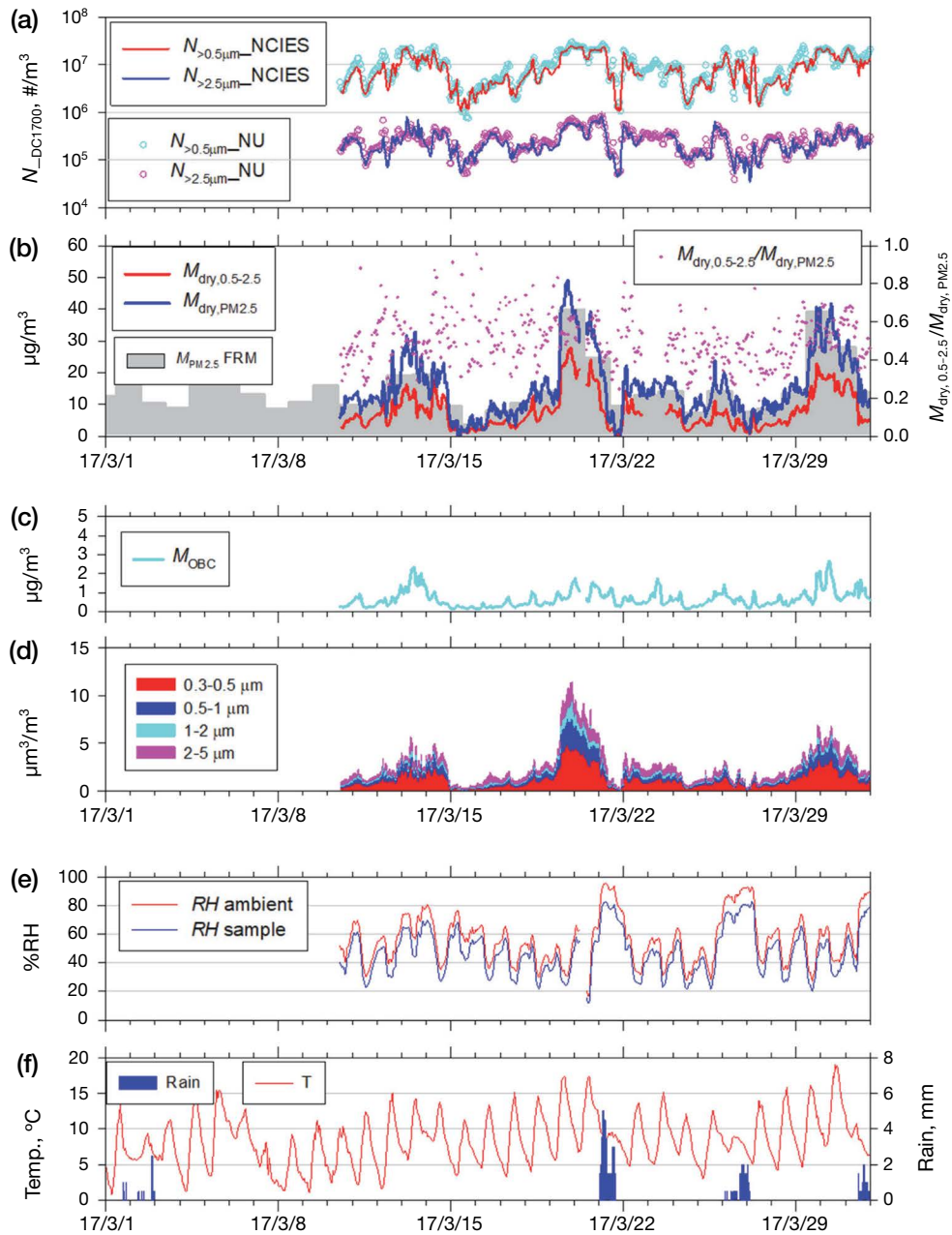


**Fig. 3.** Temporal variations are shown: (a) number concentrations found using DC1700 at NCIES and NU; (b) mass concentrations of 0.5–2.5  $\mu\text{m}$  diameter particles found using DC1700 ( $M_{\text{dry},0.5-2.5}$ ), mass concentration of PM<sub>2.5</sub> by PM712 ( $M_{\text{dry},\text{PM}_{2.5}}$ ), and by FRM ( $M_{\text{PM}_{2.5}}$  FRM), and the ratio of  $M_{\text{dry},0.5-2.5}$  and  $M_{\text{dry},\text{PM}_{2.5}}$  at NCIES; (c) mass concentration of OBC ( $M_{\text{OBC}}$ ) found using PM712; (d) volume concentrations of aerosols with 0.3–5  $\mu\text{m}$  diameter by OPC at NU; (e) relative humidity of ambient air measured at outside of PM712 ( $RH_{\text{ambient}}$ ) and downstream of the sample filter of PM712 ( $RH_{\text{sample}}$ ) at NCIES; and (f) temperature and hourly precipitation at a local meteorological observatory for March 2017.

days was a similar level ( $R^2 = 0.778$ ). Seasonal changes in detection for another low-cost sensor to measure atmospheric PM<sub>2.5</sub> also reported from results of several studies. Sayahi *et al.* (2019) measured mass concentrations of

particulate matter using PMS 1003 and 5003 at Salt Lake City, Utah, in the USA. Correlation to 24-hr averaged PM<sub>2.5</sub> mass concentration by FRM was good ( $R^2 > 0.88$ ) in winter, but poorer ( $R^2$  of 0.18–0.32) in spring. Naka-

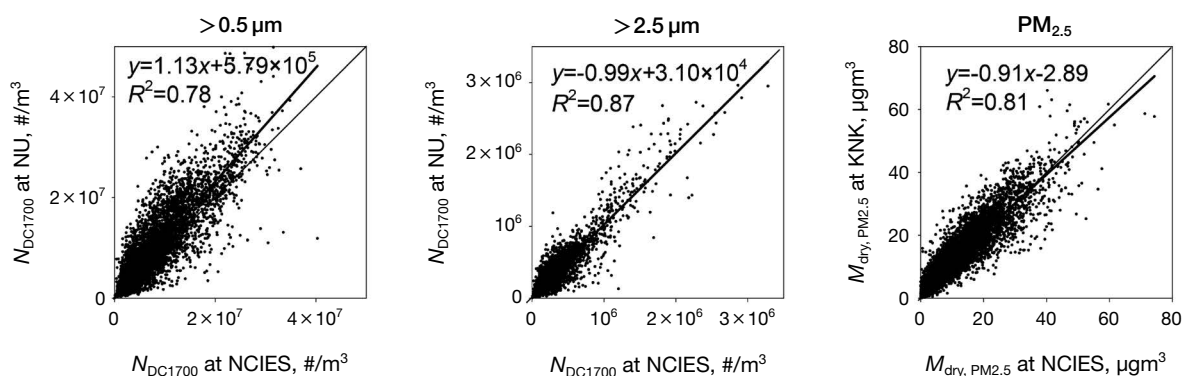


**Fig. 4.** Scatter plots of number concentrations of  $>0.5 \mu\text{m}$  and  $2.5 \mu\text{m}$  measured using DC1700 at NCIES and NU, and of the mass concentrations of  $\text{PM}_{2.5}$  at NCIES and KNK.

yama *et al.* (2017) evaluated a new palm-sized optical  $\text{PM}_{2.5}$  sensor ( $\text{PM}_{2.5}$  sensor; Panasonic Corp.) at four urban and suburban sites in Japan. Their slope to standard  $\text{PM}_{2.5}$  mass concentration tended to be higher in winter than in summer, which was inferred as attributable to small particles by photochemical formation. They also reported that the sensor tended to overestimate the  $\text{PM}_{2.5}$  mass concentration by hygroscopic growth of particles.

### 3.3 Cause of Difference between $M_{\text{dry}, 0.5-2.5}$ and $M_{\text{dry}, \text{PM}_{2.5}}$ and Seasonal Variation of $M_{\text{dry}, 0.5-2.5}/M_{\text{dry}, \text{PM}_{2.5}}$

The  $M_{\text{dry}, 0.5-2.5}$  found in this study was corrected for hygroscopic growth. Therefore, differences between  $M_{\text{dry}, 0.5-2.5}$  and  $M_{\text{dry}, \text{PM}_{2.5}}$  reflect the contribution of other factors. The  $M_{\text{dry}, 0.5-2.5}$  values were always less than those of  $M_{\text{dry}, \text{PM}_{2.5}}$ . Sousan *et al.* (2016) reported tests of the detection efficiency of DC1700 using monodispersed fine salt (0.1, 0.2 and  $0.3 \mu\text{m}$ ) and large oleic acid (1.3, 2, 3 and  $5 \mu\text{m}$ ) particles. The actual detection efficiency for the DC1700 in the size range of  $0.5-2.5 \mu\text{m}$  was 52% for  $1.3 \mu\text{m}$  particles. The difference of actual detection efficiency from manufacturer specifications can affect the underestimation of  $M_{\text{dry}, 0.5-2.5}$  to  $M_{\text{dry}, \text{PM}_{2.5}}$ . Moreover, the difference of  $M_{\text{dry}, 0.5-2.5}$  to  $M_{\text{dry}, \text{PM}_{2.5}}$  in this study tended to vary seasonally. This finding suggests that the difference can change along with the seasonal change of atmospheric aerosols. As factors affecting the seasonal change of  $M_{\text{dry}, 0.5-2.5}/M_{\text{dry}, \text{PM}_{2.5}}$ , we can infer the existence of light-absorbing particles and smaller fine particles below the detection limit, and infer a difference of size distribution in the estimation equations to that of actual atmospheric aerosols. Effects on estimation of the

mass concentration of  $\text{PM}_{2.5}$  using DC1700 and the seasonal change by each factor are explained below.

#### 3.3.1 Existence of Light-absorbing Particles

Light-absorbing particles are detected inappropriately as being of smaller size because of the lower intensity of light scattering for the same physical size of non-light-absorbing particles. According to Sousan *et al.* (2016), who described laboratory tests for DC 1700, the detected diesel exhaust particles were one or more orders fewer than those detected using non-light absorbing salts having the same mass concentration. In the present study, the average fraction of OBC mass concentrations to  $\text{PM}_{2.5}$  was  $7.8 \pm 9.5\%$  (average  $\pm$  standard deviation for this observation period). The light absorption of aerosols might partly affect underestimation at such a level. Fig. 7a, b and c present monthly box plots for  $M_{\text{dry}, \text{PM}_{2.5}}$ ,  $M_{\text{OBC}}$  and ratios of  $M_{\text{OBC}}/M_{\text{dry}, \text{PM}_{2.5}}$  at NCIES. Median values of  $M_{\text{OBC}}/M_{\text{dry}, \text{PM}_{2.5}}$  were less than 0.2 for all data (Fig. 7c). The ratios were slightly high in October with slight variation. In that year,  $M_{\text{dry}, \text{PM}_{2.5}}$  of October was lowest (Fig. 7a) because of the arrival of multiple typhoons.  $M_{\text{OBC}}$  of October was of a comparable level to the other months (Fig. 7b). Therefore, the mass fraction of black carbon was apparently high. However, comparison to  $M_{\text{dry}, 0.5-2.5}/M_{\text{dry}, \text{PM}_{2.5}}$  in Fig. 6 shows that the seasonal variation of  $M_{\text{OBC}}/M_{\text{dry}, \text{PM}_{2.5}}$  was less and was poorly matched.

#### 3.3.2 Existence of Smaller Fine Particles below the Detection Limit

The minimum size detectable by DC1700 is  $0.5 \mu\text{m}$  as the optical diameter. Earlier studies have also demonstrated the significant contribution of particles with diame-

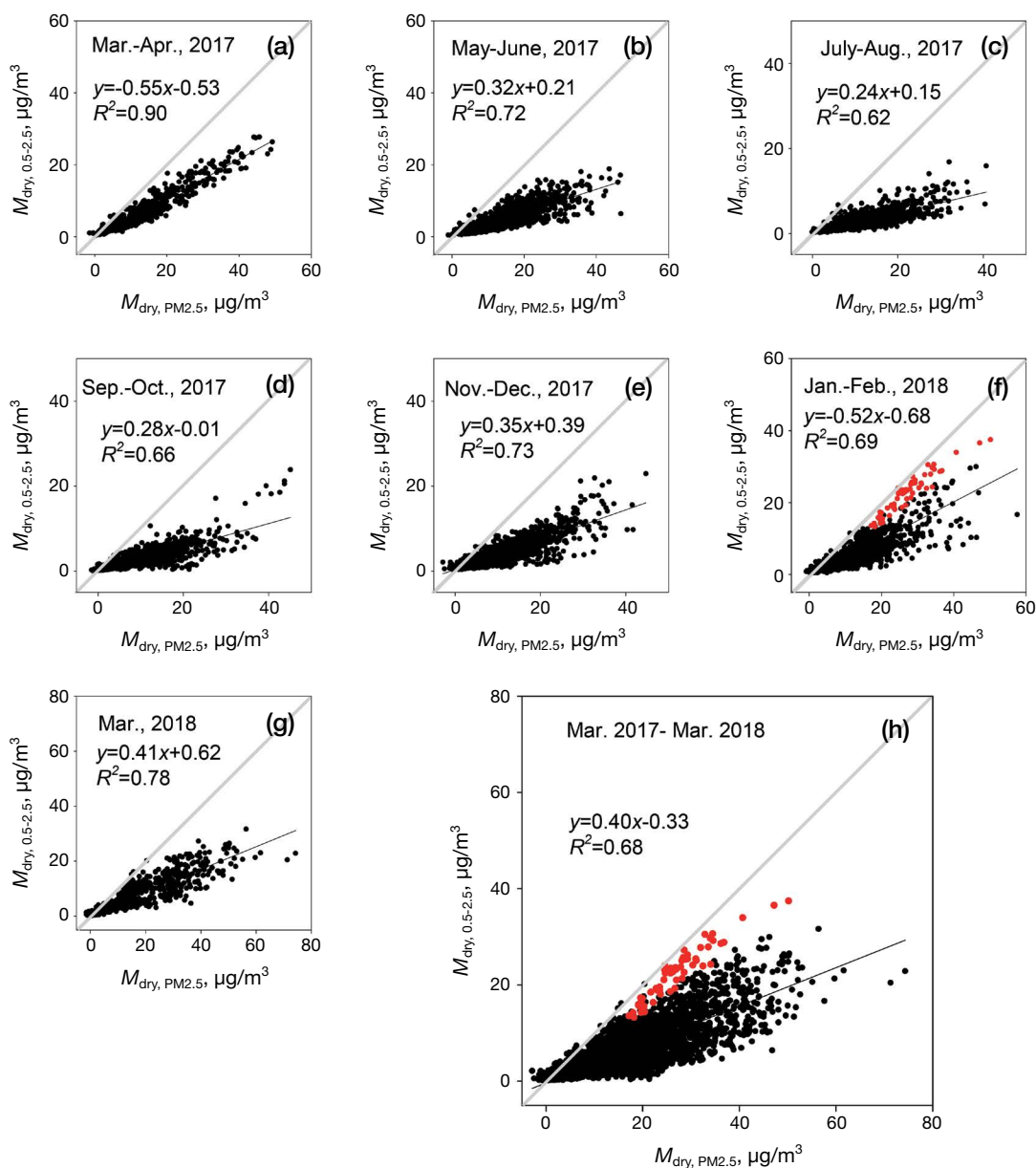


**Fig. 5.** Scatter plots of mass concentrations of 0.5–2.5 μm in diameter by DC1700 versus mass concentration of PM<sub>2.5</sub> by PM712 for two months (a–g) and for a year from Mar. 2017 through Mar. 2018. Periods of events B (18:00–19:00 20 February 2018), and C (21:00–25:00 26 February 2018) and D (16:00–20:00 28 February 2018) are denoted by red dots.

ters smaller than the detectable size limit of the DC 1700 sensor (Zikkova *et al.*, 2017; Manikoda *et al.*, 2016; Sousan *et al.*, 2016). Fig. 7d presents monthly box plots for the volume ratios of 0.5–2.0 μm to 0.3–2.0 μm ( $V_{0.5-2.0 \mu\text{m}} / V_{0.3-2.0 \mu\text{m}}$ ) by KC01D at NU. The median values were maximum (0.5) in December and minimum (0.3) in July. The seasonal variation of high values in winter and low values in summer were close to those of  $M_{\text{dry}, 0.5-2.5} / M_{\text{dry}, \text{PM}_{2.5}}$  in Fig. 6. The volume fraction of particles

smaller than 0.5 μm in PM<sub>2.5</sub> might affect the seasonal difference between  $M_{\text{dry}, 0.5-2.5}$  and  $M_{\text{dry}, \text{PM}_{2.5}}$ . Fig. 8 portrays the monthly averaged number-size distribution measured using the KC01D device at NU and their volume-size distribution for December and July 2017. For the volume-size distribution, the area of each bar for a size range corresponds to the volume concentration for the size range. Aerosol measurements were taken using the DC1700 device under ambient relative humidity.

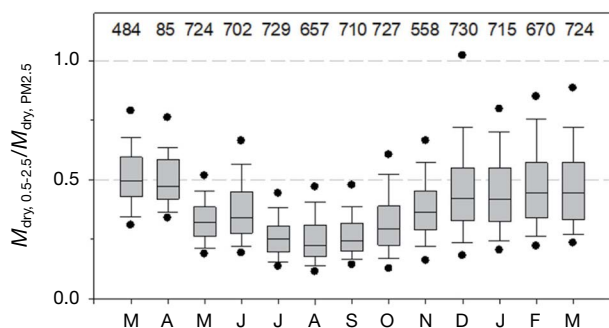


**Fig. 6.** Monthly box plots for ratio of mass concentration of 0.5–2.5  $\mu\text{m}$  by DC1700 ( $M_{\text{dry}, 0.5-2.5}$ ) to mass concentration of  $\text{PM}_{2.5}$  by PM712. The lower boundary of the box shows the 25th percentile, the line within the box represents the median, and the upper boundary of the box shows the 75th percentile. Whiskers above and below the box respectively show the 90th and 10th percentiles. Numbers shown above boxes are the numbers of observed data.

Therefore, some hygroscopic particles having less than 0.5  $\mu\text{m}$  dry diameter can be counted if the particles become larger than 0.5  $\mu\text{m}$  under ambient conditions. The dry size ( $D_{\text{dry}, 0.5}$ ) of the minimum detectable size (0.5  $\mu\text{m}$ ) by the DC1700 in ambient conditions was estimated using the hygroscopicity of ammonium sulfate (Snider *et al.*, 2016). Actually,  $D_{\text{dry}, \text{min}}$  was  $0.39 \pm 0.06 \mu\text{m}$ , on average, during the observation periods. Similarly, the dry size ( $D_{\text{dry}, 2.5}$ ) of the upper detection size (2.5  $\mu\text{m}$ ) obtained using the DC1700 device was estimated as  $1.9 \pm 0.3 \mu\text{m}$ . The  $D_{\text{dry}, 0.5}$  and  $D_{\text{dry}, 2.5}$  are shown as dashed and solid red lines in Fig. 8b.

$\text{PM}_{2.5}$  particles by PM712 were classified as less than 2.5  $\mu\text{m}$  under ambient conditions by a virtual impactor. Therefore, the size range of dried  $\text{PM}_{2.5}$  was also estimated as less than  $D_{\text{dry}, 2.5}$  (ca. 2  $\mu\text{m}$ ). Although particles less than  $D_{\text{dry}, 0.5}$  can affect underestimation of  $M_{\text{dry}, 0.5-2.5}$  to  $M_{\text{dry}, \text{PM}_{2.5}}$ , the estimated volume concentration for sizes of 0.3–2  $\mu\text{m}$  in Fig. 8b was a maximum at 0.3–0.5  $\mu\text{m}$ . The  $D_{\text{dry}, 0.5}$  was in 0.3–0.5  $\mu\text{m}$ . According to parameters for atmospheric volume-size distributions derived from averages of measurements reported by Whitby (1978), the respective mode peaks of the accumulation and coarse mode particles were 0.32  $\mu\text{m}$  and 5.7  $\mu\text{m}$  for urban aerosols. The volume fraction of particles smaller than 0.5  $\mu\text{m}$  to particles smaller than 2.5  $\mu\text{m}$  can be estimated as 62% based on Whitby’s parameters. Considering size changes attributable to hygroscopic growth, the volume fraction of particles smaller than 0.39  $\mu\text{m}$  ( $D_{\text{dry}, \text{min}}$ ) among particles smaller than 2  $\mu\text{m}$  was 54%. The result suggests that the contribution of particles smaller than the

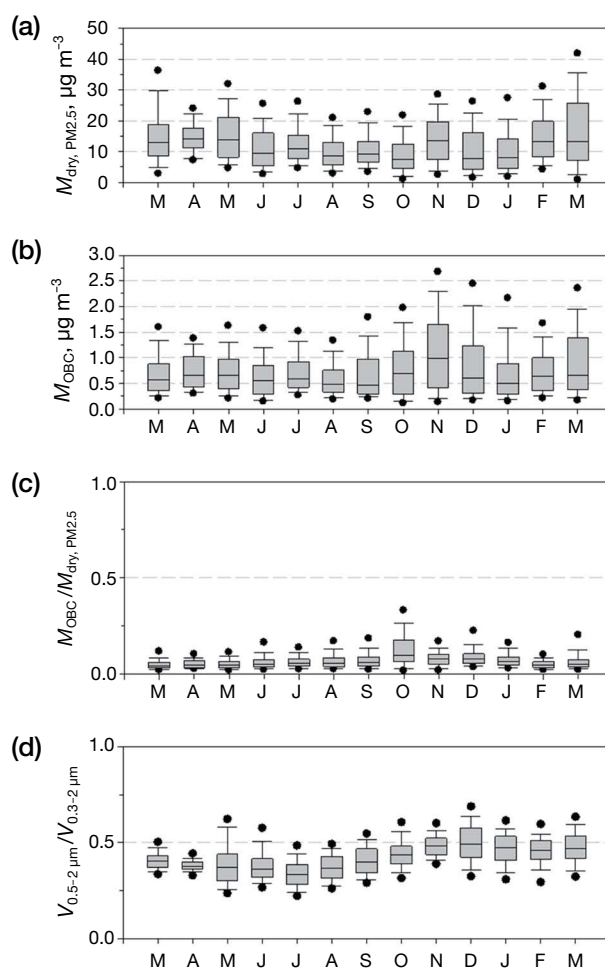


**Fig. 7.** Monthly box plots for mass concentrations of  $\text{PM}_{2.5}$  (a) and OBC (b) and the ratio of mass concentration of OBC to  $\text{PM}_{2.5}$  (c) by PM712 at NCIES and the ratio of volume concentrations of 0.5–2  $\mu\text{m}$  to 0.3–2  $\mu\text{m}$  (d) measured by OPC at NU. The lower boundary of the box shows the 25th percentile, the line within the box represents the median, and the upper boundary of the box shows the 75th percentile. Whiskers above and below the box respectively show the 90th and 10th percentiles. The numbers shown above boxes are the numbers of observed data.

detection limit especially accounts for the underestimation of  $M_{\text{dry}, 0.5-2.5}$  to  $M_{\text{dry}, \text{PM}_{2.5}}$ .

Although the volume concentration of particles smaller than 0.3  $\mu\text{m}$  was unknown for this study, the volume ratio of 0.3–0.5  $\mu\text{m}$  to 0.5–2  $\mu\text{m}$  of July 2017 was minimum (Fig. 7d). The volume fraction of particles smaller than the detection limit ( $D_{\text{dry}, 0.5}$ ) was expected to be high in July 2017; consequently, the values of  $M_{\text{dry}, 0.5-2.5} / M_{\text{dry}, \text{PM}_{2.5}}$  were small. Given a volume concentration of less than 0.3  $\mu\text{m}$  as  $V_{<0.3 \mu\text{m}}$ , the ratio of  $M_{\text{dry}, 0.5-2.5}$  to  $M_{\text{dry}, \text{PM}_{2.5}}$  was almost equivalent to the ratio of  $V_{0.5-2.0 \mu\text{m}}$  to

( $V_{<0.3 \mu\text{m}} + V_{0.3-2.0 \mu\text{m}}$ ). The ratio of  $M_{\text{dry}, 0.5-2.5}$  to  $M_{\text{dry}, \text{PM}_{2.5}}$  is expected to be somewhat larger because the DC1700 counted hygroscopic particles of less than 0.5  $\mu\text{m}$ . In consideration of general and observed volume-size distribution, we assumed simple values of  $V_{<0.3 \mu\text{m}}$ : the values of  $V_{<0.3 \mu\text{m}}$  are  $V_{0.3-2.0 \mu\text{m}}$  and  $0.5 \cdot V_{0.3-2.0 \mu\text{m}}$ , respectively, when the accumulation mode diameters are small (as in July) and large (as in December). Then, the ratios of  $V_{0.5-2.0 \mu\text{m}}$  to ( $V_{<0.3 \mu\text{m}} + V_{0.3-2.0 \mu\text{m}}$ ) were estimated respectively as 0.15 and 0.33. Consequently, the size change can become a factor of difference of 0.18 by this assumption, which was comparable to a difference of  $M_{\text{dry}, 0.5-2.5}/M_{\text{dry}, \text{PM}_{2.5}}$  between July and December (ca. 0.2) in Fig. 6. As implied by this estimate and by Whitby's size distribution, the seasonal variation of  $V_{0.5-2.0 \mu\text{m}}/V_{0.3-2.0 \mu\text{m}}$  suggests that a particle volume smaller than the detection limit of DC1700 varies with the season. The contributions of smaller particles might be greater in summer because the formation and growth of secondary particles is more active in summer (Okada, 1985). These results suggest that simple conversion of number data from Dyls to PM<sub>2.5</sub>, which is independent of the size distribution, would engender large bias, with variation derived from seasonal changes in the size distribution.

### 3.3.3 Difference of Size Distribution in the Estimation Equations to Actual Atmospheric Aerosols

From estimation of  $M_{\text{dry}, 0.5-2.5}$  using equations (2) and (3), the geometric average between 0.5 and 2.5  $\mu\text{m}$  was used as  $D$  in this study. In the equations, a  $dV/d\log D$  was

used for the size range. However, the equation is correct in theory when  $dV/d\log D$  is linear to  $\log D$  because excess volume for a size range larger than the geometric average between  $D_{\text{dry}, 0.5}$  and  $D_{\text{dry}, 2.5}$  is equal to the shortage volume for a smaller size range. For the observed volume-size distribution as presented in Fig. 8b, the volume concentration around  $D_{\text{dry}, 0.5}$  tended to be somewhat high, especially in July 2017, rather than showing a linear change. Therefore, the assumption of  $D$  in this study (i.e. a geometric average between 0.5 and 2.5  $\mu\text{m}$ ) can engender some overestimation of the actual  $M_{\text{dry}, 0.5-2.5}$ . Considering that point, the mass concentration of dried particles counted by DC1700 would be smaller than the estimated  $M_{\text{dry}, 0.5-2.5}$ , especially when the volume concentration of approximately 0.5  $\mu\text{m}$  was high. Therefore, the difference of size distribution between assumption and actual aerosols is regarded as reducing the seasonal difference of  $M_{\text{dry}, 0.5-2.5}/M_{\text{dry}, \text{PM}_{2.5}}$ , rather than the factor of the difference.

### 3.4 Example of Short-term Event Effects on a Particular Size Distribution

Fig. 9 presents temporal variations of  $M_{\text{dry}, 0.5-2.5}$ ,  $M_{\text{dry}, \text{PM}_{2.5}}$  at NCIES,  $M_{\text{dry}, \text{PM}_{2.5}}$  at KNK, and other parameters by KC01D, along with meteorological data for February 2018. As described earlier,  $M_{\text{dry}, 0.5-2.5}/M_{\text{dry}, \text{PM}_{2.5}}$  was usually about 0.4. However,  $M_{\text{dry}, 0.5-2.5}/M_{\text{dry}, \text{PM}_{2.5}}$  were occasionally higher than 0.7, with high mass concentration events such as B (18:00–8:00 20 February 2018), C (21:00–9:00 26 February 2018), and D (16:00–20:00 28 February 2018). As depicted in Fig. 9f and h

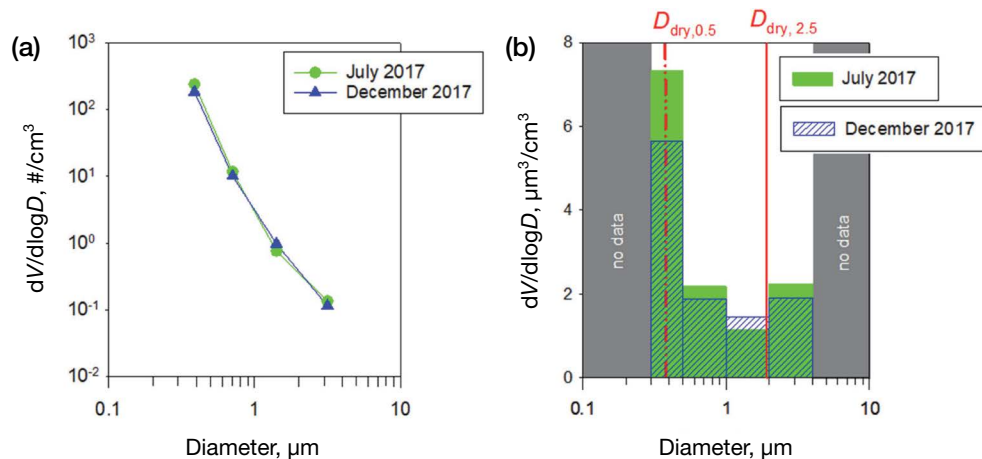


**Fig. 8.** Monthly averaged number-size distribution (a) and volume-size distributions (b) of aerosol particles by KC01D for July and December 2017. Red dash-dotted and solid lines of (b) respectively represent the yearly averaged dried size of 0.5  $\mu\text{m}$  and 2.5  $\mu\text{m}$  particles estimated by assuming ammonium sulfate.

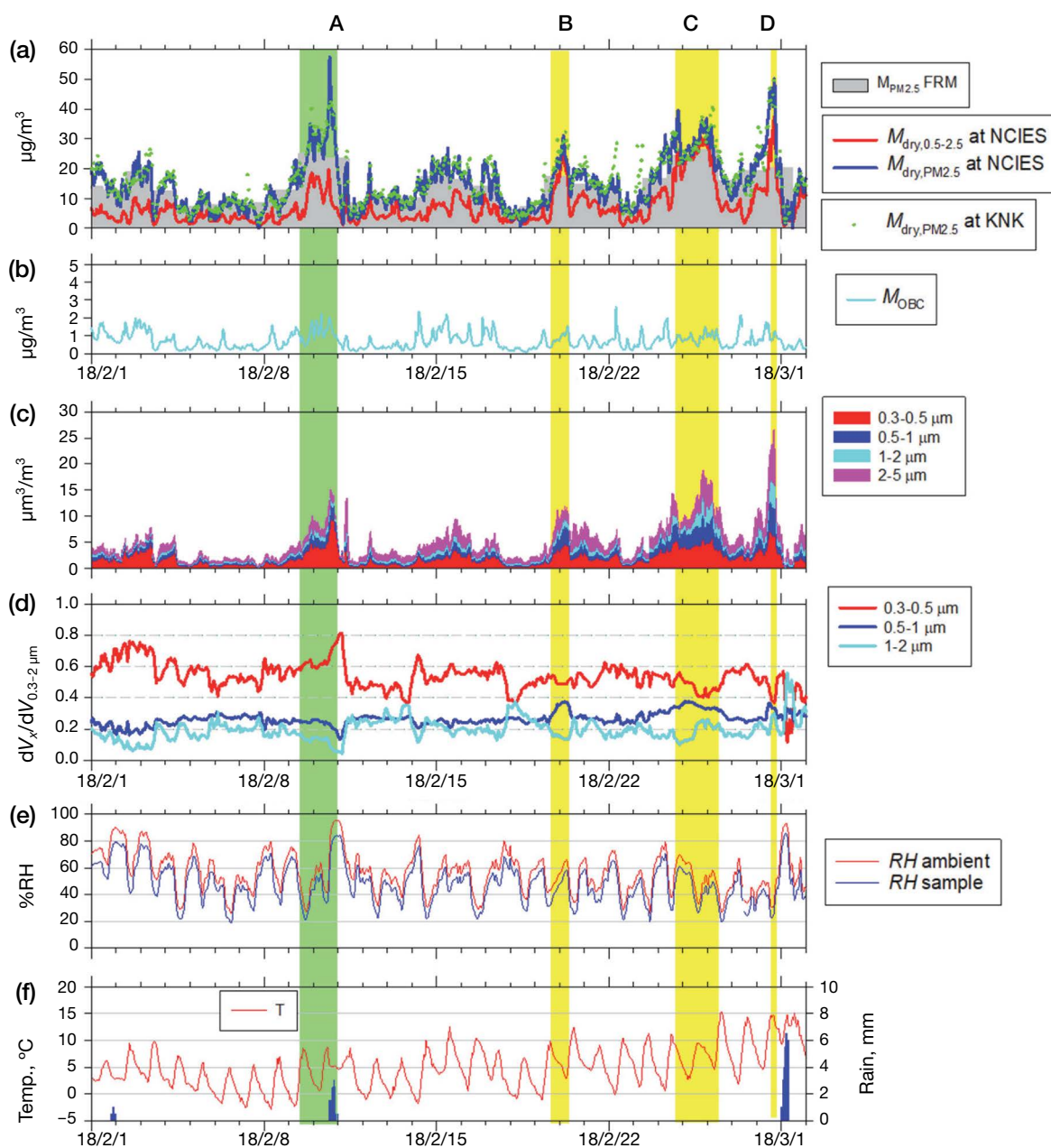


**Fig. 9.** Temporal variations are shown: (a) mass concentration of 0.5–2.5  $\mu\text{m}$  in diameter by DC1700 ( $M_{\text{dry},0.5-2.5}$ ) and mass concentrations of  $\text{PM}_{2.5}$  by PM712 and FRM ( $M_{\text{dry},\text{PM}_{2.5}}$  at NCIES and  $M_{\text{PM}_{2.5}}$  FRM) at NCIES and mass concentrations of  $\text{PM}_{2.5}$  by ASCA-14 at Kanokoden ( $M_{\text{dry},\text{PM}_{2.5}}$  at KNK); (b) mass concentration of OBC; (c) volume concentrations of aerosols with 0.3–5  $\mu\text{m}$  diameter by OPC at NU; (d) volume fractions of 0.3–0.5  $\mu\text{m}$ , 0.5–1  $\mu\text{m}$  and 1–2  $\mu\text{m}$  particles to 0.3–2  $\mu\text{m}$  particles; (e) relative humidity of ambient air ( $RH_{\text{ambient}}$ ) and downstream of sample filter of PM712 ( $RH_{\text{sample}}$ ) at NCIES; and (f) temperature and hourly precipitation at local meteorological observatory for February 2018. Periods of high-concentration events A, B, C, and D are highlighted by green and yellow bars.

with data colored in red, these high ratios of  $M_{\text{dry},0.5-2.5}/M_{\text{dry},\text{PM}_{2.5}}$  were rarely observed during the remainder of the year. For the other high mass concentration event A (8 February 2018) in Fig. 9a, the ratio of  $M_{\text{dry},0.5-2.5}/M_{\text{dry},\text{PM}_{2.5}}$  was at a normal level (ca. 0.5). Values of  $M_{\text{PM}_{2.5}}$  by

FRM and  $M_{\text{dry},\text{PM}_{2.5}}$  at KNK during events A–D also corresponded well to  $M_{\text{dry},\text{PM}_{2.5}}$  at NCIES (Fig. 9a). These increases of  $M_{\text{dry},\text{PM}_{2.5}}$  in events A–D occurred during the dry condition ( $RH_{\text{ambient}} < 70\%$ ) without precipitation (Fig. 9a, e and f).

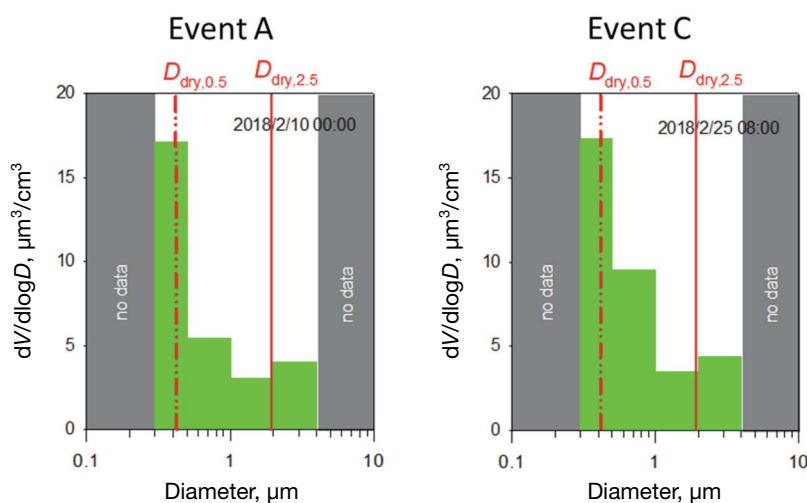


**Fig. 10.** Volume-size distributions of aerosol particles by KC01D for events A and C. Red dash-dotted and solid lines respectively show the dried sizes of 0.5  $\mu\text{m}$  and 2.5  $\mu\text{m}$  particles estimated by assuming ammonium sulfate.

As estimated in section 3.3, particles smaller than the detection limit can account for the large fraction of underestimation of  $M_{\text{dry}, 0.5-2.5}$  to  $M_{\text{dry}, PM_{2.5}}$  among some factors. Therefore, size distribution differences might affect the ratio of  $M_{\text{dry}, 0.5-2.5}$  to  $M_{\text{dry}, PM_{2.5}}$ . In events C–D, the fraction of 0.5–1.0  $\mu\text{m}$  particles (Fig. 9d) increased with higher  $M_{\text{dry}, PM_{2.5}}$ . In event A (8 February 2018), an increase of smaller (0.3–0.5  $\mu\text{m}$ ) particles contributed to the increase of  $M_{\text{dry}, PM_{2.5}}$ . For comparison, volume-size distributions of events A and C are presented in Fig. 10. As the figure shows, the volume concentration of 0.5–1.0  $\mu\text{m}$  particles of event C was clearly greater than that of event A. Therefore, the volume fraction of particles larger than  $D_{\text{dry}, 0.5}$  was apparently higher for event C. The precipitous change observed for the difference between  $M_{\text{dry}, 0.5-2.5}$  and  $M_{\text{dry}, PM_{2.5}}$  was regarded as mainly reflecting rapid changes in the volume-size distribution.

As shown in Fig. 5h, drastic events of  $M_{\text{dry}, 0.5-2.5}/M_{\text{dry}, PM_{2.5}}$  change, such as events B, C, and D, rarely occurred throughout the year. Nevertheless, these events demonstrated that a particle fraction that is undetectable by DC1700 can change drastically in a single day, not only on the time-scale of seasons. Therefore, to use DC1700 data as a proxy of atmospheric  $PM_{2.5}$ , attention must be devoted to temporal changes of the number-size distribution.

#### 4. SUMMARY AND CONCLUSIONS

To assess the usability of a low-cost optical particle

counter for measurements of atmospheric  $PM_{2.5}$ , measurements were taken using DC1700, PM712, and FRM for a year in Nagoya city, Japan. The daily average of  $M_{\text{dry}, PM_{2.5}}$  by PM712 was well correlated with the mass concentration of  $PM_{2.5}$  by FRM. The value of  $M_{\text{dry}, 0.5-2.5}$  measured using DC1700 was always less than  $M_{\text{dry}, PM_{2.5}}$  measured by PM712, but they showed good correlation (slope = 0.40,  $R^2 = 0.68$ ) for the year. The slope values of  $M_{\text{dry}, 0.5-2.5}$  to  $M_{\text{dry}, PM_{2.5}}$  tended to change seasonally: the minimum was 0.24 of July–August 2017; the maximum was 0.55 of May–April 2017.

As causes of difference between  $M_{\text{dry}, 0.5-2.5}$  and  $M_{\text{dry}, PM_{2.5}}$ , we considered some factors in addition to the detection efficiency of instruments evaluated by an earlier study: light absorbing particles, smaller fine particles with less than the minimum detection diameter, and the method of estimating  $M_{\text{dry}, 0.5-2.5}$ . The contributions of light absorption of aerosols and particles less than the minimum detection diameter were inferred respectively as ca. 8% (on average during this observation) and ca. 54% (in general). The seasonal variation of  $M_{\text{dry}, 0.5-2.5}/M_{\text{dry}, PM_{2.5}}$  apparently reflects the seasonal variation of the number-size distribution better than that of light absorbing particles. Three short-term events observed during the year changed the ratio of  $M_{\text{dry}, 0.5-2.5}$  to  $M_{\text{dry}, PM_{2.5}}$  to high values with the increase of  $M_{\text{dry}, PM_{2.5}}$ . The sporadic event affecting  $M_{\text{dry}, 0.5-2.5}$  was attributed to the increase of the detectable particle fraction with the change in the number-size distribution.

The mass concentration estimated from DC1700 sho-

wed some degree of correlation with  $PM_{2.5}$  for each of two months. Our results suggest that data conversion using a simple correction factor can provide a rough value of  $PM_{2.5}$  within a season. However, as this study demonstrated, the mass fraction of particles of undetectable size found using DC1700 was large in atmospheric  $PM_{2.5}$ . This outcome can engender underestimation or overestimation of  $PM_{2.5}$  from DC1700 data according to differences in the size distribution. Consequently, to estimate  $PM_{2.5}$  more reliably, appropriate correction of temporal changes in the size distribution should be included not only to adjust for hygroscopicity.

## ACKNOWLEDGEMENT

This work was performed with the support of a Grant-in-Aid from the Environment Research and Technology Development Fund, Grant No. 5-1604, provided by Environmental Restoration and Conservation Agency of Japan.

## REFERENCES

- Austin, E., Novosselov, I., Setom, E., Yost, M.G. (2015) Laboratory Evaluation of the Shinyei PPD42NS Low-Cost Particulate Matter Sensor. *PLOS ONE*, 10(9). <https://doi.org/10.1371/journal.pone.0137789>
- Dacunto, P.J., Klepeis, N.E., Cheng, K.-C., Acevedo-Bolton, V., Jiang, R.-T., Repace, J.L., Ott, W.R., Hildemann, L.M. (2015) Determining  $PM_{2.5}$  Calibration Curves for a Low-Cost Particle Monitor: Common Indoor Residential Aerosols. *Environmental Science: Processes & Impacts*, 17, 1959-1966. <https://doi.org/10.1039/C5EM00365B>
- EPA (2013) National Ambient Air Quality Standards for Particulate Matter; Final Rule, Federal Register of Environmental Protection Agency, USA, 78, 3086-3287.
- Han, I., Symanski, E., Stock, T.H. (2017) Feasibility of using low-cost portable particle monitors for measurement of fine and coarse particulate matter in urban ambient air. *Journal of the Air & Waste Management Association*, 67(3), 330-340. <https://doi.org/10.1080/10962247.2016.1241195>
- Hasegawa, S., Yamagami, M., Suzuki, Y., Kumagai, K., Nishimura, R. (2018) Verification of measured values by  $PM_{2.5}$  automatic measuring instruments using the standard method. *Journal of Environmental Laboratories Association*, 43(1), 40-46 (in Japanese). [http://tenbou.nies.go.jp/science/institute/region/journal/JELA\\_4301040\\_2018.pdf](http://tenbou.nies.go.jp/science/institute/region/journal/JELA_4301040_2018.pdf)
- Ikemori, F., Honjyo, K., Yamagami, M., Nakamura, T. (2015) Influence of contemporary carbon originating from the 2003 Siberian forest fire on organic carbon in  $PM_{2.5}$  in Nagoya, Japan. *Science of Total Environment*, 530-531, 403-441. <https://doi.org/10.1016/j.scitotenv.2015.05.006>
- Iwamoto, Y., Sekine, H., Saito, S., Miura, K., Nishikawa, M., Nagano, K., Osada, K. (2018) Continuous measurement of hygroscopic characteristics of  $PM_{2.5}$  using an optical particle counter - Including case analysis of high concentration events in December 2016. *Eaerosoru Kenkyu*, 33(4), 238-247. <https://doi.org/10.11203/jar.33.238>
- Jayarathne, R., Liu, X., Thai, P., Dunbabin, M., Morawska, L. (2018) The influence of humidity on the performance of a low-cost air particle mass sensor and the effect of atmospheric fog. *Atmospheric Measurement Techniques*, 11(8), 4883-4890. <https://doi.org/10.5194/amt-11-4883-2018>
- Jiao, W., Hagler, G., Williams, R., Sharpe, R., Brown, R., Garver, D., Judge, R., Caudill, M., Rickard, J., Davis, M., Weinstock, L., Zimmer-Dauphinee, S., Buckley, K. (2016) Community Air Sensor Network (CAIRSENSE) project: evaluation of low-cost sensor performance in a suburban environment in the southeastern United States. *Atmospheric Measurement Techniques*, 9(11), 5281-5292. <https://doi.org/10.5194/amt-9-5281-2016>
- Johnson, K., Bergin, M.H., Russell, A.G., Hagler, G.S.W. (2018) Field Test of Several Low-Cost Particulate Matter Sensors in High and Low Concentration Urban Environments. *Aerosol and Air Quality Research*, 18, 565-578. <http://www.aaqr.org/doi/10.4209/aaqr.2017.10.0418>
- Jones, S., Renée Anthony, T., Sousan, S., Altmaier, R., Park, J.H., Peters, T.M. (2016) Evaluation of a Low-Cost Aerosol Sensor to Assess Dust Concentrations in a Swine Building. *The Annals of Occupational Hygiene*, 60(5), 597-607. <https://doi.org/10.1093/annhyg/mew009>
- Jovašević-Stojanović, M., Bartonova, A., Topalović, D., Lazović, I., Pokrić, B., Ristovski, Z. (2015) On the use of small and cheaper sensors and devices for indicative citizen-based monitoring of respirable particulate matter. *Environmental Pollution*, 206, 696-704. <https://doi.org/10.1016/j.envpol.2015.08.035>
- Kelly, K.E., Whitaker, J., Petty, A., Widmer, C., Dybwad, A., Sleeth, D., Martin, R., Butterfield, A. (2017) Ambient and laboratory evaluation of a low-cost particulate matter sensor. *Environmental Pollution*, 221, 491-500. <https://doi.org/10.1016/j.envpol.2016.12.039>
- Kulkarni, P., Baron, P.A., Willeke, K. (2011) *Aerosol Measurement: Principles, Techniques, and Applications*, Third ed., John Wiley & Sons, Inc. Hoboken, NJ, 883pp.
- Kumar, P., Morawska, L., Martani, C., Biskos, G., Neophytou, M., Di Sabatino, S., Bell, M., Norford, L., Britter, R. (2015) The rise of low-cost sensing for managing air pollution in cities. *Environment International*, 75, 199-205. <https://doi.org/10.1016/j.envint.2014.11.019>
- Lelieveld, J., Evans, J.S., Fnais, M., Giannadaki, D., Pozzer, A. (2015) The Contribution of Outdoor Air Pollution Sources to Premature Mortality on a Global Scale. *Nature*, 525, 367-371. <https://www.nature.com/articles/nature15371>
- Liu, D., Zhang, Q., Jiang, J., Chen, D.-R. (2017) Performance calibration of low-cost and portable particulate matter (PM) sensors. *Journal of Aerosol Science*, 112, 1-10. <https://doi.org/10.1016/j.jaerosci.2017.05.011>
- Manikonda, A., Zíková, N., Hopke, P.K., Ferro, A.R. (2016)

- Laboratory assessment of low-cost PM monitors. *Journal of Aerosol Science*, 102, 29–40. <https://doi.org/10.1016/j.jaerosci.2016.08.010>
- Nakayama, T., Matsumi, Y., Kawahito, K., Watabe, Y. (2017) Development and evaluation of a palm-sized optical PM<sub>2.5</sub> sensor. *Aerosol Science and Technology*, 52(1), 2–12. <https://doi.org/10.1080/02786826.2017.1375078>
- Rai, A.C., Kumar, P., Pilla, F., Skouloudis, A.N., Sabatino, S.D., Ratti, C., Yasar, A., Rickerby, D. (2017) End-user perspective of low-cost sensors for outdoor air pollution monitoring. *Science of The Total Environment*, 607–608, 691–705. <https://doi.org/10.1016/j.scitotenv.2017.06.266>
- Sayahi, T., Butterfield, A., Kelly, K.E. (2019) Long-term field evaluation of the Plantower PMS low-cost particulate matter sensors. *Environmental Pollution*, 245, 932–940. <https://doi.org/10.1016/j.envpol.2018.11.065>
- Semple, S., Ibrahim, A.E., Apsley, A., Steiner, M., Turner, S. (2013) Using a new, low-cost air quality sensor to quantify second-hand smoke (SHS) levels in homes. *Tobacco Control*, 24(2). <https://doi.org/10.1136/tobaccocontrol-2013-051188>
- Slowik, J.G., Stainken, K., Davidovits, P., Williams, L.R., Jayne, J.T., Kolb, C.E., Worsnop, D.R., Rudich, Y., DeCarlo, P.F., Jimenez, J.L. (2004) Particle Morphology and Density Characterization by Combined Mobility and Aerodynamic Diameter Measurements. Part 2: Application to Combustion-Generated Soot Aerosols as a Function of Fuel Equivalence Ratio. *Aerosol Science and Technology*, 38(12), 1206–1222. <https://doi.org/10.1080/027868290903916>
- Snider, G., Weagle, C.L., Murdymootoo, K.K., Ring, A., Ritchie, Y., Stone, E., Walsh, A., Akoshile, C., Anh, N.X., Balasubramanian, R., Brook, J., Qonitan, F.D., Dong, J., Griffith, D., He, K., Holben, B.N., Kahn, R., Lagrosas, N., Lestari, P., Ma, Z., Misra, A., Norford, L.K., Quel, E.J., Salam, A., Schichtel, B., Segev, L., Teipathi, S., Wang, C., Yu, C., Zhang, Q., Zhang, Y., Brauer, M., Cohen, A., Gibson, M.D., Liu, Y., Martins, J.V., Rudich, Y., Martin, R.V. (2016) Variation in global chemical composition of PM<sub>2.5</sub>: emerging results from SPARTAN. *Atmospheric Chemistry and Physics*, 16, 9629–9653. <https://doi.org/10.5194/acp-16-9629-2016>
- Sousan, S., Koehler, K., Thomas, G., Park, J.H., Hillman, M., Halterman, A., Peters, T.M. (2016) Inter-comparison of low-cost sensors for measuring the mass concentration of occupational aerosols. *Aerosol Science and Technology*, 50(5), 462–473. <https://doi.org/10.1080/02786826.2016.1162901>
- Ueda, K., Yamagami, M., Ikemori, F., Hisatsune, K., Nitta, H. (2016) Associations Between Fine Particulate Matter Components and Daily Mortality in Nagoya, Japan. *Journal of Epidemiology*, 26(5), 249–257. <https://doi.org/10.2188/jea.JE20150039>
- Yamagami, M., Ikemori, F., Nakashima, H., Hisatsune, K., Osada, K. (2019) Decreasing trend of elemental carbon concentration with changes in major sources at Mega city Nagoya, Central Japan. *Atmospheric Environment*, 199, 155–163. <https://doi.org/10.1016/j.atmosenv.2018.11.014>
- Zhang, Q., Jiang, X., Tong, D., Davis, S.J., Zhao, H., Geng, G., Feng, T., Zheng, B., Lu, Z., Streets, D.G., Ni, R., Brauer, M., van Donkelaar, A., Martin, R.V., Huo, H., Liu, Z., Pan, D., Kan, H., Yan, Y., Lin, J., He, K., Guan, D. (2017) Transboundary Health Impacts of Transported Global Air Pollution and International Trade. *Nature*, 543, 705–709. <https://www.nature.com/articles/nature21712>
- Zheng, T., Bergin, M.H., Johnson, K.K., Tripathi, S.N., Shirodkar, S., Landis, M.S., Sutaria, R., Carlson, D.E. (2018) Field evaluation of low-cost particulate matter sensors in high- and low-concentration environments. *Atmospheric Measurement Technology*, 11, 4823–4846. <https://doi.org/10.5194/amt-11-4823-2018>
- Zikova, N., Masiol, M., Chalupa, D.C., Rich, D.Q., Ferro, A.R., Hopke, P.K. (2017) Estimating hourly concentrations of PM<sub>2.5</sub> across a metropolitan area using low-cost particle monitors. *Sensors*, 17(8), 1922. <https://doi.org/10.3390/s17081922>